ChemComm

Accepted Manuscript

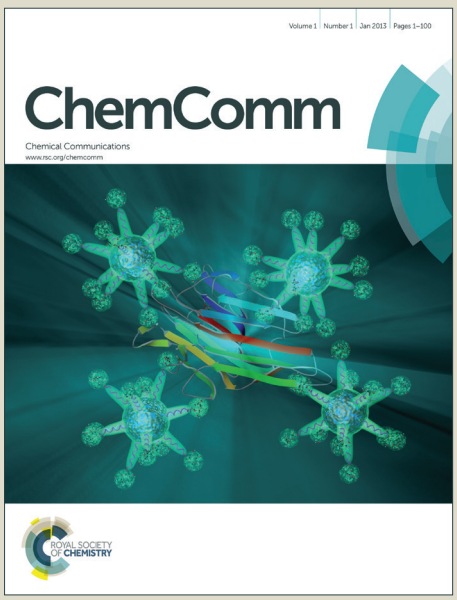

ROYAL SOCIETY OF CHEMISTRY

www.rsc.org/chemcomm

Journal Name

RSCPublishing

COMMUNICATION

Thiol-modified Gold Nanoparticles for the Inhibition of *Mycobacterium smegmatis*

Cite this: DOI: 10.1039/x0xx00000x

Jennifer C. Gifford,[a] Jamee Bresee,[a] Carly Jo Carter,[a] Guankui Wang,[a] Roberta J. Melander,[b] Christian Melander,[b] and Daniel L. Feldheim[a]

Received 00th January 2012,
Accepted 00th January 2012

DOI: 10.1039/x0xx00000x

www.rsc.org/

Antimicrobial drug discovery has slowed considerably over the last few decades. One major cause for concern is the lack of innovative approaches to treat infections caused by mycobacteria such as TB. Herein we demonstrate that our Small Molecule Variable Ligand Display (SMLVD) method for nanoparticle antibiotic discovery can be expanded around a ligand feed ratio parameter space to identify gold nanoparticle conjugates that are potent inhibitors of mycobacteria growth, with our most potent inhibitor able to reduce growth by five orders of magnitude at 8 μM.

Antimicrobial drug resistance has become one of the most serious threats to global health to emerge in the 21st century. For example, approximately 11,000 people die annually in the United States from methicillin-resistant *Staphylococcus aureus* (MRSA) infections.[1, 2] Additionally, the World Health Organization (WHO) estimates that there are over 1.3 million deaths each year due to *Mycobacterium tuberculosis* (TB) infections, with approximately 170,000 deaths due to multidrug resistant (MDR) strains.[3] As of September 2013, extensively-drug resistant (XDR) TB accounted for 10% of all MDR-TB diagnoses, with 92 countries having one or more reported cases.[4] As these numbers continue to grow, novel strategies for discovering antibiotics that access new bacterial targets and are able to avoid current resistance mechanisms are desperately needed.

To address the need for antibiotics that are less susceptible to the resistance mechanisms that can quickly compromise small-molecule antibiotics, our labs have developed a new paradigm in drug discovery called small molecule variable ligand display (SMVLD). In SMVLD, combinations of small organothiol ligands are attached to gold nanoparticles to create a library of mixed-ligand modified nanoparticle conjugates that are subsequently screened for bacterial growth inhibition activity. Using a modest set of 10 commercially available organothiols, we previously assembled a library of 120 different mixed thiol/gold nanoparticle conjugates. Certain thiol combinations were shown to be potent growth inhibitors of *Escherichia coli*, *S. aureus*, and *Klebsiella pneumoniae*.[5, 6] Nanoparticle activity was shown to depend upon the specific combination of ligands attached to the particle surface and, with a 99.9% minimum inhibitory concentration ($MIC_{99.9}$) of 250 nM for *E. coli*, the nanoparticles that we have developed are more potent toward *E. coli* inhibition than many small-molecule antibiotics on the market currently, such as ampicillin (11 μM), gentamicin (1 μM), and chloramphenicol (12 μM).[7, 8] Furthermore, we have shown that *E. coli* develops resistance against the nanoparticles far more slowly than against the small-molecule drug chloramphenicol.[9]

Herein we show that one of the most potent nanoparticle conjugates for *E. coli* growth inhibition could be modified for use in *M. smegmatis* growth inhibition. As *M. smegmatis* is frequently considered to be a non-pathogenic surrogate for TB,[9-11] the results reported here suggest that mixed ligand monolayer/gold nanoparticle conjugates may also have the potential to serve as a next generation TB antibiotic.

A SMVLD library of 120 nanoparticle conjugates was screened previously for *E. coli* growth inhibition, and several potent hits were discovered. One conjugate, LAL-33, which displayed on its surface pMBA plus ligands **6**, **8**, and **9** (Figure 1), was shown to have a $MIC_{99.9}$ of 500 nM (where we define $MIC_{99.9}$ as growth

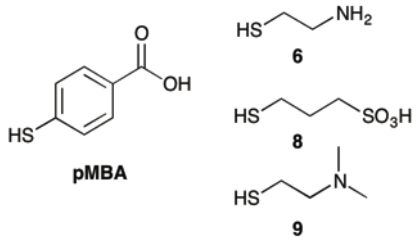

Figure 1. Chemical structures of 4-mercaptobenzoic acid (pMBA), cysteamine (6), 3-mercapto-1-propane sulfonic acid (8) and 2-diethylaminoethane thiol (9).

reduction by 99.9% in comparison to the untreated bacterial control growth). To investigate whether this conjugate had broad-spectrum activity, it was tested against *M. smegmatis* using plating and colony count analysis. LAL-33 showed no activity against *M. smegmatis* up to 10 μM, the highest concentration tested (Table 1). However, an important feature of SMVLD is that the activity of a lead conjugate may be further optimized simply by adjusting the ratio of thiol ligands attached to the gold nanoparticle surface; we were thus interested in exploring whether this simple approach could turn LAL-33 from an inactive nanoparticle formulation to one with growth inhibition activity towards *M. smegmatis*. We therefore re-screened LAL-33 around an expanded "feed ratio" parameter space, where the feed ratio is the mole ratio of thiol:gold nanoparticles input into the ligand exchange reaction. LAL-33 is prepared using a feed ratio of 46:1 for thiol **6**, and 33:1 for thiols **8** and **9**. As a result of this expanded search several potent new conjugates were identified (Table 1). A feed ratio of 46:1 for all three thiols yielded the most potent conjugate, resulting in an $MIC_{99.9}$ of 6 μM and a minimal bactericidal concentration (MBC) of 8 μM (we define the MBC as the lowest concentration that provides 5 logs or 99.999% of growth inhibition vs. untreated control). This conjugate is designated LAL-3346.

Table 1. Results of an expanded feed ratio screen performed to identify new nanoparticle conjugates with *M. smegmatis* growth inhibition activity.

Conjugate Name	Feed Ratio, Thiol **6**	Feed Ratio, Thiol **8**	Feed Ratio, Thiol **9**	% Inhibition	Inhibitory Concentration, μM
LAL-33	46	33	33	N/A	>10
LAL-3316	46	46	16	83.7	8
LAL-3333	46	46	33	99.1	8
LAL-3346	46	46	46	99.9	6

To determine whether *M. smegmatis* growth inhibition was due to the thiol/gold nanoparticle conjugate or if activity could be recapitulated by the free ligands alone, different combinations of **6**, **8**, and **9** were mixed in solution and screened for activity. As we have noted for other bacteria, no combination of free thiols in solution was active against *M. smegmatis* up to a total thiol concentration of 1 mM. Nanoparticle conjugates were also synthesized with various combinations of only one or two of the ligands. These conjugates were also inactive up to the highest concentration tested, 10 μM. Nanoparticles with only the original pMBA ligand attached showed no activity at any concentration up to 50 μM. We therefore conclude that the specific combination of thiols **6**, **8**, and **9** and the conjugation of these thiols to the nanoparticle surface using a specific feed ratio are necessary for growth inhibition.

The presence of all three ligands in relative specific amounts was confirmed previously by solid-state NMR.[9] In brief, those studies showed qualitatively that all ligands input into the exchange reaction were present on LAL-33 and LAL-3346, and that the ratio of **8** to **6** increased from LAL-33 to LAL-3346 as would be expected by the increase in feed ratio. These results indicate that adjusting the ligand feed ratio does affect the ratio of ligands bound to the surface of the nanoparticle.

LAL-3346 was characterized further by transmission electron microscopy (TEM). TEM images of pre- (pMBA-only modified particles) and post-exchanged nanoparticles revealed a change in core diameter from 2.7 nm ± 0.8 nm to 1.6 nm ± 0.6 nm. From this result, it was concluded that post-exchange particles were smaller than pMBA-gold nanoparticles, but similarly monodispersed in size (Supplemental Information). LAL-33, LAL-3316, and LAL-3333 (the inactive or less active conjugates from Table 1) were also measured to rule out if the smaller size was conferring activity. In all cases, post-exchange nanoparticles were the same size within standard deviation as LAL-3346, despite varying degrees of activity towards *M. smegmatis* (Supplemental Information). This indicated that the size reduction that occurred during the exchange reaction, which is likely the result of Au etching,[13] was not responsible for antibacterial activity. Similarly, the presence of thiols **6**, **8,** and **9** on the surface of these smaller nanoparticles is not sufficient to cause growth inhibition of *M. smegmatis*; instead, it was determined that the specific feed ratios of this ligand combination were responsible for growth inhibition of *M. smegmatis*.

The specificity of LAL-3346 for *M. smegmatis* vs. other bacteria was tested using *E. coli*, *K. pneumoniae*, and methicillin-resistant *S. aureus*, as well as two non-TB mycobacteria *M. abscessus* and *M. avium*. There was no significant activity towards any of these species with the exception of *E. coli*, which had an $MIC_{99.9}$ of 500 nM as mentioned previously.

Several experiments were then performed to investigate the mode of action of these particles. As with the *E. coli* inhibitors published previously,[5] LAL-3346 nanoparticles contain the cationic ligands **6** and **9**, which have the potential to disrupt cell membranes.[14, 15] Therefore, a membrane permeability assay was completed first using the LIVE/DEAD BacLight Bacterial Viability kit from Invitrogen. *M. smegmatis* was incubated with LAL-3346 particles ranging in concentration from 1 μM to 16 μM and the degree of membrane permeabilization compared to an untreated control was determined to be between 11% and 17%, respectively (Supplemental Information). Such low percentages indicate that disruption of the membrane is unlikely to be a significant mode of

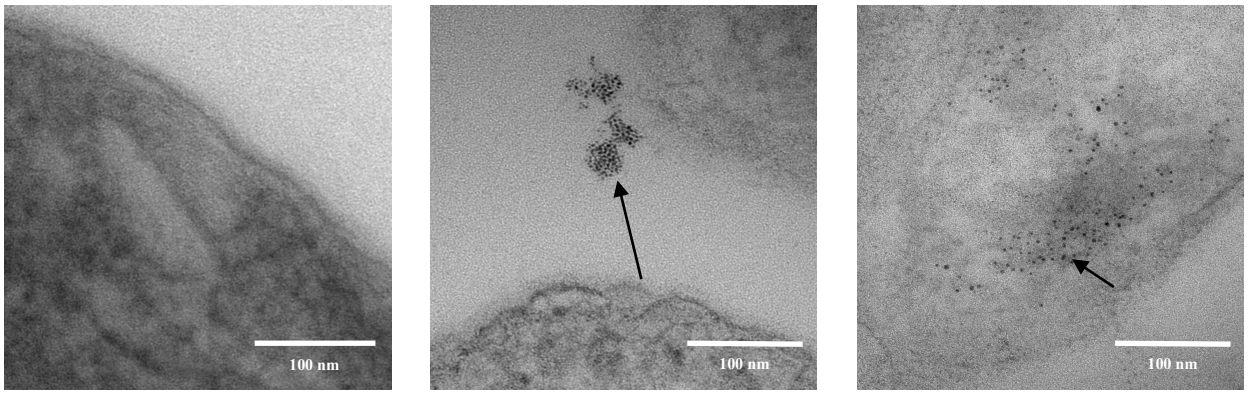

Figure 2. Transmission electron micrographs of untreated *M. smegmatis* (left panel), *M. smegmatis* treated with pMBA-gold nanoparticles (middle panel) and *M. smegmatis* treated with LAL-3346 nanoparticles (right panel). The arrows indicate the edge of the cell membrane at their tails and the location of the nanoparticles at their points.

action of nanoparticle activity.

We then employed a BacLight Bacterial Membrane Potential stain and flow cytometry to investigate any changes in membrane potential that might be induced due to the presence of pMBA or LAL-3346 nanoparticles (Supplemental Information). In comparison to the negative control – stained but untreated mycobacteria – LAL-3346 was observed to have a similar cellular membrane potential. However, pMBA nanoparticles behaved similarly to the positive control in the experiment, carbonyl cyanide 3-chlorophenylhydrazone, a reagent that reduces membrane potential by eliminating proton gradients. These experiments indicated that pMBA-gold nanoparticles affect the membrane potential without causing growth inhibition or cell death, while LAL-3346 nanoparticles affect cell growth but do not alter the membrane potential.

In order to gain further insight into the interactions between gold nanoparticles and *M. smegmatis*, nanoparticles were incubated with *M. smegmatis* cells. The cells were then pelleted, washed to remove un-associated nanoparticles, and imaged by TEM. The images show pMBA-gold nanoparticle conjugates clumped together outside of the mycobacterial cell membrane, potentially providing a mechanistic basis for the disrupted membrane potential. In contrast, LAL-3346 nanoparticles were found to be internalized into the mycobacteria (Figure 2). The potential therefore exists for LAL-3346 to affect *M. smegmatis* growth by interacting with intracellular biomolecular targets. The origin of these targets will be explored in the future with a DNA microarray analysis.

Finally, it was of interest to determine if LAL-3346 is toxic to mammalian cells. This was accomplished by performing a hemolysis assay in which nanoparticles were incubated with defibrinated sheep's blood cells. In 24 hours, the relative EC_{50} of LAL-3346 was determined to be 8.3 μM. The hemolytic index for this conjugate, defined as the $EC_{50}/MIC_{99.9}$, was thus 1.4. A second toxicity experiment was performed with MRC-5 human lung cells (ATCC CCL-171). However, we were unable to obtain a complete dose-response curve even when increasing the nanoparticle concentration to 100 μM (Supplemental Information), which suggests that LAL-3346 is significantly less toxic towards lung cells than blood cells.

In conclusion, we have successfully applied our SMVLD method to the discovery of active nanoparticle conjugates for *M. smegmatis* growth inhibition, as illustrated in Figure 3. The most active mixed thiol/gold nanoparticle conjugate, LAL-3346, was discovered simply by expanding the ligand "feed ratio" space around a ratio (LAL-33) that yielded active conjugates for *E. coli* inhibition. Remarkably, by slightly adjusting the feed ratio of two out of three thiols in the ligand exchange reaction, we were able to transition from a ligand composition that was inactive toward *M. smegmatis* to one that was highly potent (LAL-3346). This result adds significantly to our previous understanding of the nanoscale structure-activity relationships (NSAR) of these nanoparticles, which was in part that both the combination of ligands and their attachment to the nanoparticle surface is necessary for activity. As a result of this work, we now know that the specific density of ligands should also be considered when formulating highly active antibiotic nanostructures. We have also shown that LAL-3346 does not simply alter the membrane permeability or membrane potential, but appears to be internalized, which suggests that intracellular targets may be accessed by gold nanoparticles. Unfortunately, this new nanoparticle formulation demonstrates toxicity towards red blood cells; however, we have shown that mammalian cell toxicity can be attenuated by nanoparticle PEGylation.[9] We are currently exploring this approach to mitigate potential *in vivo* toxicity. In an era of necessity, our nanoparticle exchange method and its success towards the non-pathogenic TB surrogate *M. smegmatis* provides a potential innovative pathway for the development of new antibiotics against challenging bacterial pathogens.

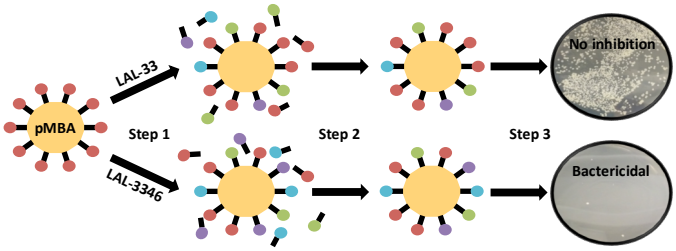

Figure 3. Schematic of the overall SMVLD method and its application to LAL-33 vs. LAL-3346, with the resulting *M. smegmatis* growth inhibition. Step 1 describes the initial SMVLD exchange reaction. In the second step, exchanged nanoparticles are purified, washed and concentrated. Finally, each nanoparticle type is incubated with *M. smegmatis* and percent growth inhibition is determined by plating and colony counting (step 3).

The authors wish to thank the Bill and Melinda Gates Foundation, NIH and the University of Colorado for financial support. They also would like to acknowledge the role of Theresa Nahreini of the University of Colorado in the mammalian cell culture and flow cytometry experiments.

Notes and references

[a] Department of Chemistry and Biochemistry, University of Colorado, Boulder, CO 80309.

[b] Department of Chemistry, North Carolina State University, Raleigh, NC 27695-8024.

Electronic Supplementary Information (ESI) available: detailed experimental methods, TEM images, size distribution measurements, membrane permeability and membrane potential data, and EC_{50} curves. See DOI: 10.1039/c000000x/

1 Center for Disease Control and Prevention. Antibiotic resistance threats in the United States, 2013.
2 R. Klevens, M. Morrison, and J. Nadle, *Jama*, 2007, **298 (15)**, 1763.
3 World Health Organization. Global Tuberculosis Report 2013, 2013.
4 World Health Organization. Multidrug-resistant tuberculosis (MDR-TB). http://www.who.int/tb/challenges/mdr/mdr_tb_factsheet.pdf?ua=1 (accessed February 20, 2014).
5 J. Bresee, K.E. Maier, C. Melander, and D.L. Feldheim, *Chemical Communications*, 2010, **46 (40)**, 7516.
6 J. Bresee, K.E. Maier, A. Boncella, C. Melander, and D.L. Feldheim, *Small*, 2011, **7 (14)**, 2027.
7 J.M. Andrews, *Journal of antimicrobial chemotherapy*, 2001, **48 (1)**, 5.
8 D. Corogeanu, R. Willmes, M. Wolke, G. Plum, O. Utermöhlen, and M. Krönke, *BMC microbiology*, 2012, **12**, 160.
9 J. Bresee, C.M. Bond, R.J. Worthington, C.A. Smith, J.C. Gifford, C.A. Simpson, C.J. Carter, G. Wang, J. Hartman, N.A. Osbaugh, R.K. Shoemaker, C. Melander, and D.L. Feldheim, *Journal of American Chemical Society,* 2014, **136 (14)**, 5295.
10 J.M. Reyrat, and D. Kahn, *Trends in* Microbiology, 2001, **9 (10)**, 472.
11 J.S. Tyagi, and D. Sharma, *Trends in Microbiology*, 2002, **10 (2)**, 68.

12 A.K. Mishra, N.N. Driessen, B.J. Appelmelk, and G.S. Besra. *FEMS microbiology reviews,* 2011, **35 (6)**, 1126.
13 T. Schaaff, R. Whetten, *J. Phys. Chem. B.*, 1999, **103**, 9394.
14 S. Hong, A. U. Bielinska, A. Mecke, B. Keszler, J. L. Beals, X. Shi, L. Balogh, B. G. Orr, J. R. Baker, M. M. Banaszak Holl, *Bioconjugate Chemistry,* 2004, **15 (4)**, 774.
15 P. R. Leroueil, S. A. Berry, K. Duthie, G. Han, V. M. Rotello, D. Q. McNerny, J. R. Baker, B. G. Orr, M. M. B. Holl, *Nano Letters.* 2008, **8 (2)**, 420.